JCSE The Journal of Corrosion Science and Engineering
ISSN 1466-8858 Volume 14, Preprint 23 submitted 3 June 2011

Investigation of Anticorrosive Property of Henna Extract for N80 API Steel in Regular Mud Acid (HCl/HF 12/3 %)

R. Abdollahi, S.R. Shadizadeh*

Department of Petroleum Engineering, Abadan Faculty of Petroleum Engineering, Petroleum University of Technology, Abadan, Iran.

*Address Correspondence to Seyed Reza Shadizadeh, Department of Petroleum Engineering, Abadan Faculty of Petroleum Engineering, Petroleum University of Technology, Northern Bowarde, Abadan, Iran, 6318714331. Email: shadizadeh@put.ac.ir

Abstract

The inhibitive action of henna extract on corrosion of N80 API steel in regular mud acid (HCL/HF 12/3 wt %) at 28, 40, 60 and 75 °C was investigated through electrochemical techniques. Polarization measurements indicate that all examined compound act as a mixed inhibitor and inhibitor efficiency increases with henna concentration. Maximum inhibition efficiency (average value) of henna extract at 28, 40, 60 and 75 ºC is 85.98, 87.21, 88.74 and 92.59 %, respectively. Obtained thermodynamic parameters indicate that adsorption of henna extract on N80 API steel in regular mud acid is spontaneous and occurs via a chemical adsorption mechanism.

Keywords: Acid Corrosion, Steel, EIS, Polarization, Weight loss

1. Introduction

In the fracturing and acidizing of compact oil formations, dilute hydrochloric and hydrofluoric acid use to dissolve the undesirable carbonate and silica deposits or scales, which interfere with the passage of oil in tubing or in the formation itself. Hydrochloric acid is an inorganic acid and is the most common acid uses in the oil well acidizing. HF uses in combination with HCI and has

The Journal of Corrosion Science and Engineering
ISSN 1466-8858 Volume 14, Preprint 23 submitted 3 June 2011

been referred to as "intensified acid" or "mud removal" acid, depending on the formulation and use. The most common mixture uses in sandstone acidizing is regular mud acid (HCL/HF 12/3 wt%). HF uses primarily to remove clay-particle damage in sandstone formations, to improve permeability of clay-containing formations, and to increase solubility of dolomite formations [1]. The lines and tubing must be protected during this operation from corrosive attack by the acid. Therefore, the use of corrosion inhibitors to prevent metal dissolution will be inevitable. A great number of scientific studies have been dedicated to the subject of corrosion inhibitors for oil well casing and tubing in acidic media [2-5].

A number of organic compounds are known to be applicable as corrosion inhibitors for steel in acidic environments. Such compounds typically contain nitrogen, oxygen or sulphur in a conjugated system and function via adsorption of the molecules on the metal surface, creating a barrier to corrodent attack [6].

Although many synthetic compounds show inhibitive action, most of them are toxic. There is increasing concern about the toxicity of corrosion inhibitors in petroleum industry. The toxic effects not only affect living organisms but also poison the earth [7]. Therefore, finding natural occurring substances as corrosion inhibitor is subject of great practical significance.

A few studies have investigated the anticorrosive property of henna extract on some metals such as aluminium, iron, zinc and nickel in acidic and alkaline solutions [7-10]. In the present work, inhibitive action of henna extract as a cheap, ecofriendly and naturally occurring substance on corrosion behavior of N80 API steel in regular mud acid (HCL/HF 12/3 % weight) at 28, 40, 60 and 75 °C was investigated through immersion test, polarization measurements and electrochemical impedance spectroscopy method.

2. Experimental

2.1. Preparation of henna extract

Henna leaves were crushed and extracted in boiled water for 2 h. The extracted solution was then filtered and concentrated until its water evaporates. This solid extract was used to study the corrosion inhibition properties and to prepare the required concentrations of henna [4].

2.2. Specimen preparation

N80 API steel specimens having nominal chemical composition of 0.36 % C, 0.27 % Si, 1.57 % Mn, 0.02 % P, 0.14 % V and Fe balance were used. Coupons were cut into 6×1.5×0.3 cm dimensions used for weight loss measurements, whereas specimens with 1.5×1×3 cm dimensions, sealed by polyester resin, leaving a surface area of 1.5 cm^2, used for working electrode for polarization and EIS measurements. Prior to carrying out the corrosion tests, the metal specimens were mechanically ground successively with, 220, 400, 800, 1000 and 1200 grade of emery paper, de-greased with acetone and rinsed by distilled water.

2.3. Solution preparation

Mud acid solution was prepared by mixture of HCL with ammonium bifluoride. One liter of regular mud acid (HCl/HF 12/3 wt %) was prepared by mixture of 959 ml HCL 15.4 % with 46 gr ammonium bifluoride.

The concentration range of henna extract employed was varied from 0.1 to 1.6 g/l. HF acid has corrosive effect on glassy apparatus and cannot be used in glassy experimental instruments. Therefore all apparatus that contact with HF acid were comprised of plastic or Teflon materials.

2.4. Weight loss measurements

Experiments were performed with different concentration of henna extract for 8 hr at 28 ºC and 1 hr at 40, 60 and 70 ºC.

The percentage inhibition efficiency (*IE %*) was calculated using the following relation:

$$IE\% = \left(\frac{W_1 - W_2}{W_1} \right) \times 100 \quad (1)$$

Where: W_2 and W_1 are the weight losses of N80 API steel in the presence and absence of inhibitor, respectively.

2.5. Electrochemical impedance spectroscopy (EIS)

Electrochemical measurements were carried out in a conventional three electrode glass cell, containing 300 ml of electrolyte at the temperature of 28, 40, 60 and 75 °C. As previously mentioned, in media that HF acid exists, use of glassy apparatus is not recommended. Therefore Teflon material electrodes were used. The working electrode, embedded in polyester resin, had a geometric area of 1.5 cm^2. Platinum electrode was used as a counter electrode and a saturated calomel electrode (SCE) as the reference electrode.

Electrochemical impedance spectroscopy measurement were performed with Autolab potentiostat PGSTAT 302 N (Eco Chemie, Utrecht, The Netherlands) driven by Frequency Response Analyzer data processing software (FRA software version 4.9). Frequency ranging was selected between 100 MHz and 10 kHz and peak to peak a.c. amplitude of 10 mV was used for calculation of polarization resistance values (R_p) and the double layer capacitance (C_{dl}). Data obtained by EIS measurement is expressed graphically in a Nyquist plot. The inhibition efficiency IE % was calculated using the following relation:

$$IE\% = \left(\frac{R_2 - R_1}{R_2} \right) \times 100 \quad (2)$$

Where R1 and R2 are the polarization resistance of N80 steel in the absence and presence of inhibitor, respectively.

2.6. Polarization measurements

Electrochemical measurements were carried out in a conventional three electrode glass cell with the same electrodes used in EIS measurements at the temperature of 28, 40, 60 and 75 °C. All electrochemical experiments were carried out using an Autolab potentiostat PGSTAT 302 N (Eco Chemie, Utrecht, The Netherlands) driven by the General Purpose Electrochemical Systems data processing software (GPES, software version 4.9). Cathodic and anodic polarization curves were recorded at a rate of 1 mV/s in a range of 200 mV more than OCP and 200 mV less than OCP.

Before recording the solution was de-aerated for 30 min and the working electrode was maintained at its corrosion potential for 25 min, until a steady state was obtained.

The inhibition efficiency IE % was calculated using the following relation:

$$\% IE = \frac{I_0 - I}{I_0} \times 100 \qquad (3)$$

Where: I and I_0 are the corrosion current densities of carbon steel in the presence and absence of inhibitor, respectively.

3. Results and discussion

3.1. Weight loss measurements

The corrosion rate and inhibition efficiency for N80 API steel immersed in regular mud acid (HCL/HF 12/3 wt %) at 28, 40, 60 and 75 °C in various concentrations of henna extract were determined. Values of corrosion rate and inhibition efficiencies are given in Table 1. It is clear from Table 1 that corrosion rate decreases more and more with the increase of henna extract.

Inhibition efficiency greatly increases with the increase of henna concentration up to 84.21 % at 1.6 g/L of henna extract at 28 °C. As the temperature increase, the inhibition efficiency increases. At 40, 60 and 75 °C maximum inhibition efficiency of 84.21, 87.50 and 89.92 % were obtained in regular mud acid (HCL/HF 12/3 wt %) solution containing 1.4 , 0.8 and 0.4 g/l henna extract, respectively. More than these optimum henna extract at each temperature, inhibition efficiency increase is not considerable. Results show that this plant extract is capable enough to reduce corrosion rate of N80 API steel immersed in regular mud acid (HCL/HF 12/3 wt %) solution in the temperature range 28–75 °C. The increase in corrosion rate is more seen with the rise of temperature for the uninhibited acid solution. This phenomenon results in increasing of inhibition efficiency at higher temperature. The presence of inhibitor leads to decrease of the corrosion rate.

3.2. EIS Experiments

The corrosion behavior of N80 API steel immersed in regular mud acid (HCL/HF 12/3 wt %) solution at 28, 40, 60 and 75 °C in various concentrations of henna extract was investigated by EIS experiments; and the optimum concentration at each temperature was determined. Obtained Data by EIS measurements is expressed graphically in a Nyquist plot. Fig. 1 through 4 show the result of EIS experiment in the Nyquist representation at 28, 40, 60 and 75 °C, respectively. After analyzing the Nyquist representation of EIS experiment, it is concluded that the curves approximated by a single capacitive semi-circle, showing that corrosion process was mainly charge transfer controlled [11]. The Nyquist plots are analyzed in terms of equivalent circuit composed with classic parallel capacitor and resistor. The impedance parameters (Polarization resistance (R_p), double layer capacitance (C_{dl}) and inhibition efficiency (IE %)) are given in Table 2. By temperature increasing, polarization resistance decreases markedly and the amount of double layer capacitance increases. The C_{dl} values are found to decrease noticeably in the presence of inhibitor, indicating the adsorption of inhibitor on metal surface in acidic media.

The Journal of Corrosion Science and Engineering
ISSN 1466-8858 Volume 14, Preprint 23 submitted 3 June 2011

The increase in the polarization resistance leads to an increase in inhibition efficiency. The results show that by temperature increasing the inhibition efficiency increases .The general shape of the curves is very similar for all samples at any temperature; the shape is maintained throughout the whole concentration, indicating that almost no change in the corrosion mechanism occurred due to the inhibitor addition.

There is a good agreement between efficiency value obtained by EIS technique and the other two methods (weight loss and polarization, polarization results are discussed in next section). It is conclude that the corrosion mechanism is electrolyte dependent and not depend on applied technique.

3.3. Polarization measurements

After determination of optimum concentration of henna extract as a corrosion inhibitor by weight lost and EIS test, polarization test was performed at 28, 40, 60 and 75 °C in two mediums as follows:

1. Uninhibited acid (Regular mud acid without any concentration of henna extract).
2. Regular mud acid with optimum concentration of henna extract (Optimum concentration of henna extract at 28, 40, 60 and 75 °C is 1.6, 1.4, 0.8 and 0.4 g/l, respectively.

The potentiodynamic anodic and cathodic polarization curves for N80 API steel immersed in regular mud acid (HCL/HF 12/3 wt %) in the absence and presence of optimum concentration of henna extract at 28, 40, 60 and 75 °C are shown in Fig. 5 through 8, respectively. Current density of each polarization curves at each temperature and concentration is determined by intersection of cathodic Tafel slope and vertical line passes through E_{Corr} point. The corrosion parameters including corrosion current density (I_{corr}), corrosion potential (E_{corr}), cathodic Tafel slope ($\cap_c$) and inhibition efficiency (IE %) are given in Table 3 at each temperature. It is illustrated from

JCSE The Journal of Corrosion Science and Engineering
ISSN 1466-8858 Volume 14, Preprint 23 submitted 3 June 2011
the data of Table 3 that by addition of henna extract the corrosion current density decreases. Also it can be clearly seen that as the temperature increases the inhibition efficiency of henna extract increases. The results show that in the presence of henna extract the value of corrosion potential increases.

3.4. Adsorption isotherms behavior

Adsorption isotherms are very important in understanding the mechanism of inhibition of corrosion reaction of metals and alloys. The most frequently used adsorption isotherms are Frumkin, Temkin, Freundlich, Flory Huggins, Bockris -Swinkel, El-Awardy and Langmuir isotherms [6].

Attempts to fit data obtained from weight loss measurement into different adsorption isotherms reveal that the data best fitted with Langmuir adsorption isotherm. Assumptions of Langmuir relate the concentration of the inhibitor in the bulk of the electrolyte (C_{inh}) to the degree of surface coverage (N) defined by IE%/100 according to equation below:

$$\frac{C_{inh}}{\theta} = \frac{1}{K} + C_{inh} \qquad (4)$$

Where: K is the equilibrium constant of adsorption.

Surface coverage values (θ) for the inhibitor were obtained from the weight loss measurements for various concentration at different temperatures, as shown in Table 1. By plotting values of $\frac{C_{inh}}{N}$ versus values of C_{inh}, straight-line graphs were obtained (Fig. 9), which proves that Langmuir adsorption isotherm is obeyed. This confirms that the adsorption behavior of the inhibitor is strongly influenced by temperature. The slopes of the $\frac{C_{inh}}{N}$ versus C_{inh} plots show deviation from unity, which means non-ideal simulating and unexpected from the Langmuir adsorption isotherm [12]. They might be the results from the interactions between the adsorbed species on the N80 API steel surface [13-14]. K values were calculated from the intercept of straight line by $\frac{C_{inh}}{N}$ axis and are given in Table 4. These data (Table 4) reveal that as the temperature increases the equilibrium constant for the adsorption process increases. This could be due to the chemisorption of henna molecules on the metal surface in which by increasing the temperature, K and consequently adsorption tendency of inhibitor on steel surface will be increased [7].

On the other hand, increasing the temperature increases the inhibition efficiency due to increased adsorption of the inhibitor [15].

The adsorption constant, *K*, is related to the standard free energy of adsorption, ΔG_{ads}, with the following equation [16]:

$$K = \frac{1}{55.5}\exp\left(-\frac{\Delta G_{ads}}{RT}\right) \quad (5)$$

Where: 55.5 is the water concentration of solution in mol/l [16]. The standard free energy of adsorption (ΔG_{ads}) values was calculated and is given in Table 4.

The negative values of ΔG_{ads} ensure the spontaneity of the adsorption process and stability of the adsorbed layer on the steel surface.

The dependence of ΔG_{ads} on temperature can be explained by two cases as follows [7]:

a) ΔG_{ads} may increase with increase of temperature, indicating the occurrence of exothermic process.

b) ΔG_{ads} may decrease with increase of temperature, indicating the occurrence of endothermic process.

Therefore, the decrease of ΔG_{ads} with temperature reveals that the inhibition of N80 API steel by henna extract is an endothermic process. In an endothermic process adsorption was favorable with increase of temperature due to the inhibitor adsorption on the steel surface [17].

The thermodynamic parameters ΔH_{ads} and ΔS_{ads} for the adsorption of henna on N80 API steel can be calculated from the following equation:

$$\Delta G_{ads} = \Delta H_{ads} - T\Delta S_{ads} \tag{6}$$

Where: ΔH_{ads} and ΔS_{ads} are the variation of enthalpy and entropy of the adsorption process, respectively. Fig. 10 shows the dependence of ΔG_{ads} on T which indicates an appropriate relationship between thermodynamic parameters. The positive sign of ΔH_{ads} reveals that the adsorption of inhibitor molecules is an endothermic process. The values of ΔS_{ads} in the presence of henna extract are large and positive, meaning that an increasing in disordering takes place in going from reactants to the metal-adsorbed species reaction complex [18].

In order to study the effect of temperature on the corrosion reaction of N80 API steel in the presence of henna extract as an inhibitor, Arrhenius equation was used [7]:

$$\log W = \log A - \left(\frac{E_a}{2.303RT} \right) \tag{7}$$

Where: E_a is the activation energy of the reaction in J/mol, T is the temperature in K, A is Arrhenius pre-exponential factor and R is the universal gas constant (8.314 J/K mol). W is the corrosion rate, obtained from Table1.

By plotting log (W) versus (1/2.303RT), the values of E_a can be calculated from the slope of the obtained straight lines (Fig. 11).

The values of E_a for N80 API steel in regular mud acid (HCL/HF 12/3 wt %) in the absence and presence of different concentration of henna extract was calculated and recorded in Table 5. Values of E_a ranged from 27.71 to 6.849 kJ/mol.

The addition of inhibitor leads to abrupt decrease in the apparent activation energy to a value lower than that of the uninhibited solution and follows by monotonous decrease with increase of inhibitor concentration (Table 5), indicating that the inhibitory action of henna extract for N80 API steel corrosion in regular mud acid media occurs via chemisorptions [19].

An alternative formulation of the Arrhenius equation is the transition state equation [20].

$$\log\frac{W}{T}=\left[\left(\log\frac{R}{hN}\right)+\left(\frac{\Delta S^*}{2.303R}\right)\right]-\frac{\Delta H^*}{2.303RT} \qquad (8)$$

Where: h is Planck's constant, N is Avogadro's number, ∞S^* is the entropy of activation and ∞H^* is the enthalpy of activation.

Figure 12 shows the plot of log (W/T) against (1/2.303RT). Straight lines are obtained with a slope of $-\infty H^*$, and by intercept of straight line with log (W/T)-axis; ∞S^* values were calculated and are given in Table4.

The negative signs of the enthalpies (∞H^*) reflect the exothermic nature of the steel dissolution process (Table 5). Large and negative values of entropies (∞S^*) imply that the activated complex in the rate determining step represents an association rather than a dissociation step, meaning that a decrease in disordering takes place on going from reactants to the activated complex [21].

3.5. Mechanism of inhibition

The results of weight loss, potentiodynamic polarization and EIS measurements show that, corrosion of N80 API steel in regular mud acid is retarded in the presence of different concentrations of the henna extract. The results clearly showed that the inhibition mechanism involves blocking of N80 API steel surface by inhibitor molecules via adsorption.

The values of thermodynamic parameters for the adsorption of inhibitors can provide valuable information about the mechanism of corrosion inhibition. While an endothermic adsorption process ($\infty H^{*} > 0$) is attributed unequivocally to chemisorption, an exothermic adsorption process ($\infty H^{*} < 0$) may involve either physisorption or chemisorption or a mixture of both the processes [18]. In the present case, the calculated values of the ∞H^{*} are greater than zero; therefore the adsorption indicating that this inhibitor can be considered chemically adsorbed.

It has been reported that henna leaves contain solouble matter, lawasone (2-Hydroxy-l, 4-naphthoquinone), resin, tannin, coumarins, gallic acid and sterols [7]. The main components of lawsonia extract are hydroxy aromatic compounds such as tannin and lawsone. The inhibitive action of tannin attributes to the formation of a passivating layer of tannates on the metal surface [22]. Tannins are also known to form complex compounds with different metal cations, especially in the basic media. For this reason they are used in the manufacture of anti-rusting paints and coating. Therefore, formation of tannins complexes may be responsible for the observed inhibition in the alkaline medium [10]. The main constituent of Henna extract is Lawsone. The structure of Lawsone is shown in scheme 1. It contains benzene unit, p-benzoquinone unit and phenolic group. Chemically, the molecule of lawsone is 2-hydroxy-1, 4-naphthoquinone [23].

Lawsone molecule is a ligand that can chelate with various metal cations forming complex compounds. Therefore, the formation of insoluble complex compounds, by combination of the metal cations and the lawsone molecules adsorbed on the metal surface, is a probable interpretation of the observed inhibition action of lawsone [7].

In the acidic medium, derealization of the lone pair of electrons on hydroxyl group takes place resulting in the rearrangement shown in scheme 2. Such a rearrangement, in the presence of metal cations, enhances the complex formation reaction. This could be the reason for the observed high inhibition efficiencies in the acidic medium for C-steel. A substantial support for the formation of metal complex is often obtained by conductometric titration [7].

4. Conclusions

Inhibition efficiency of henna extract as a corrosion inhibitor for N80 API steel in regular mud acid at 28, 40, 60 and 75 ºC is 85.98, 87.21, 88.74 and 92.59 %, respectively; therefore henna extract has admissible inhibition efficiency for inhibition of N80 API steel in regular mud acid in the range of 28-75 ºC. The results show that by temperature increasing the inhibition efficiency of henna extract on N80 API steel in regular mud acid increases.

Adsorption analysis confirms that inhibition effect of henna was performed via the chemical adsorption of henna molecules on the steel surface and adsorption follows the Langmuir isotherm.

References:

[1] G.R. Coulter and A.R. Jennings, A contemporary approach to matrix acidizing, SPE Production & Facilities14 (1999) 144-149.

[2] A. Rostami and H.A. Nasr-EI-Din, Review and evaluation of corrosion inhibitors used in well stimulation", SPE paper No. 121726 , Presented at the 2009 SPE International Symposium on Oilfield Chemistry held in The Woodlands, Texas, USA, 20-22 April, 2009.

[3] S. Vishwanatham and N. Haldar, Furfuryl alcohol as corrosion inhibitor for N80 API steel in

hydrochloric acid", Corros. Sci. 50 (2008) 2999-3004.

[4] S. Vishwanatham and P.K. Sinha, Corrosion protection of N80 steel in HCl by condensation products of aniline and phenol, Anti-Corros. Method M. 56 (2009) 139-144.

[5] M.A. Quraishi and D. Jamali, Fatty acid triazoles: Novel corrosion inhibitors for oil well steel (N-80) and mild steel", J. AM. Oil Chem. Soc. 77 (2000) 1107-1111.

[6] E.E. Ebenso, N.O. Eddy and A.O. Odiongenyi, Corrosion inhibition and adsorption properties of methocarbamol on mild steel in acidic medium", Portugaliae Electrochimca. Acta 27 (2009) 13-22.

[7] A. Ostovari, S.M. Hoseinieh, M. Peikari, S.R. Shadizadeh and S.J. Hashemi, Corrosion inhibition of mild steel in 1 M HCl solution by henna extract: a comparative study of the inhibition by henna and its constituents (lawsone, gallic acid, α-d-glucose and tannic acid), Corros. Sci. 51 (2009) 1935-1949.

[8] H. Al-Sehaibani, Evaluation of extracts of henna leaves as environmentally friendly corrosion inhibitors for metals, Materialwiss. Werkst. 31 (2000) 1060-1063.

[9] A. Chetouani and B. Hammouti, Corrosion inhibition of iron in hydrochloric acid solutions by naturally henna", Bull. Electrochem. 19 (2003) 23-25.

[10] A.Y. El-Etre, M. Abdallah and Z.E. El-Tantavy, Corrosion inhibition of some metals using lawsonia extract", Corros. Sci. 47 (2005) 385-395.

[11] R. Rosliza, W.B Wan Nik and H.B. Senin, The effect of inhibitor on the corrosion of aluminum alloys in acidic solutions", Mater. Chem. Phys. 107 (2008) 281-288.

[12] W.A. Badawy, K.M. Ismail and A.M. Fathi, Corrosion control of Cu-Ni alloys in neutral chloride solutions by amino acids, Electrochim. Acta 51 (2006) 4182-4189.

[13] M.A. Migahed, H.A. Mohammed and A.M. Al-Sabagh, Corrosion inhibition and adsorption

properties of methocarbamol on mild steel in acidic medium", Mater. Chem. Phys. 80 (2003) 169-175.

[14] A. Azim, L.A. Shalaby and A. Abbas, Mechanism of the corrosion inhibition of Zn anode in NaOH by gelatine and some inorganic anions, Corros. Sci. 14 (1974) 21-24.

[15] K.C. Emregül and M. Hayvali, Studies on the effect of a newly synthesized Schiff base compound from phenazone and vanillin on the corrosion of steel in 2 M HCl. Corros. Sci. 48 (2006) 797-812.

[16] J. Flis and T. Zakroczymski, Impedance study of reinforcing steel in simulated pore solution with tannin, Electrochem. Soc. 143 (1996) 2458-2464.

[17] E.A. Noor, Temperature effects on the corrosion inhibition of mild steel in acidic solutions by aqueous extract of fenugreek leaves", Int. J. Electrochem. Sci 2 (2007) 996-1017.

[18] F. Bentiss, M. Lebrini and M. Lagrenee, Thermodynamic characterization of metal dissolution and inhibitor adsorption processes in mild steel/2,5-bis(n-thienyl)-1,3,4-thiadiazoles/hydrochloric acid cystem, Corros. Sci. 47 (2005) 2915-2931.

[19] E. Chaieb, A. Bouyanzer, B. Hammouti and M. Benkaddour, Inhibition of the corrosion of steel in 1 M HCl by eugenol derivatives, App. Surf. Sci. 246 (2005) 199-206.

[20] M. Abdallah, Ethoxylated fatty alcohols as corrosion inhibitors for dissolution of zinc in hydrochloric acid", Corros. Sci. 45 (2003) 2705-2716.

[21] S. Martinez and I. Stern, Thermodynamic characterization of metal dissolution and inhibitor adsorption processes in the low carbon steel/mimosa tannin/sulfuric acid system, Appl. Surf. Sci. 199 (2002) 83-89.

[22] G.H. Boot and S.J. Mercer, The effect of mimosa tannin on the corrosion of mild steel in the presence of sulphate-reducing bacteria, Corros. Sci. 4 (1964) 425-433.

[23] S. Rajendran, M. Agasta, R. Bamadevi, B. Shyamaladev, K. Rajam and J. Jeyasundari, Corrosion inhibition by an aqueous extract of henna leaves (lawsonia inermis L)", Zaštita materijala 50 (2009) 77-84.

Fig. 1. Nyquist plots for N80 API steel in regular mud acid (HCL/HF 12/3 wt %) at 28 °C containing different concentrations of henna extract.

Fig. 2. Nyquist plots for N80 API steel in regular mud acid (HCL/HF 12/3 wt %) at 40 ºC containing different concentrations of henna extract.

Fig. 3. Nyquist plots for N80 API steel in regular mud acid (HCL/HF 12/3 wt %) at 60 ºC containing different concentrations of henna extract.

Fig. 4. Nyquist plots for N80 API steel in regular mud acid (HCL/HF 12/3 wt %) at 75 ºC containing different concentrations of henna extract.

Fig. 5. Polarization curves for N80 API steel in regular mud acid (HCL/HF 12/3 wt %) in the absence and presence of optimum concentration of henna extract (1.6 g/l) at 28 ºC.

Fig. 6. Polarization curves for N80 API steel in regular mud acid (HCL/HF 12/3 wt %) in the absence and presence of optimum concentration of henna extract (1.4 g/l) at 40 ºC.

Fig. 7. Polarization curves for N80 API steel in regular mud acid (HCL/HF 12/3 wt %) in the absence and presence of optimum concentration of henna extract (0.8 g/l) at 60 ºC.

Fig. 8. Polarization curves for N80 API steel in regular mud acid (HCL/HF 12/3 wt %) in the absence and presence of optimum concentration of henna extract (0.4 g/l) at 75 ºC.

Fig. 9. Adsorption isotherm of henna on N80 API steel surface in regular mud acid (HCL/HF 12/3wt %) solution at different temperatures.

Fig. 10. Variation of ΔG_{ads} versus T on N80 API steel in regular mud acid (HCL/HF 12/3 wt %) containing different values of henna extract.

Fig. 11. Arrhenius plots of the corrosion rate for N80 API steel in regular mud acid (HCL/HF 12/3 wt %) solution.

Fig. 12. Arrhenius plots of the corrosion rates in regular mud acid.

Table 1

Corrosion rate and inhibition efficiency of N80 API steel immersed in regular mud acid (HCL/HF 12/3 wt %) at 28, 40, 60 and 75 °C.

Table 2

Impedance parameters of N80 API steel in regular mud acid (HCL/HF 12/3 wt %) at 28, 40, 60 and 75°C containing different concentrations of henna extract.

Table 3

Kinetic parameters of N80 API steel in regular mud acid (HCL/HF 12/3 wt %) at 28, 40, 60 and75 ± 1°C containing optimum concentrations of henna extract and blank acid.

Table 4

Surface coverage, equilibrium constant and thermodynamic parameters for the adsorption of henna on N80 API steel surface in regular mud acid (HCL/HF 12/3 %) at different temperatures.

Table 5

Activation parameters for N80 API steel corrosion in regular mud acid solutions containing different concentrations of henna extract.

Table 1

Corrosion rate and inhibition efficiency of N80 API steel immersed in regular mud acid (HCL/HF 12/3 wt %) at 28, 40, 60 and 75 °C.

Medium (g/l)	W (mg/cm^2 h)	IE (%)	θ
Temperature (k) = 301.15			
0	1.56	-	-
0.2	0.60	61.01	0.6101
0.4	0.57	63.00	0.6300
0.6	0.45	70.70	0.7070
0.8	0.42	72.50	0.7250
1	0.37	76.33	0.7633
1.2	0.33	78.46	0.7846
1.4	0.29	81.20	0.8120
1.6	0.27	84.21	0.8421
Temperature (k) = 313.15			
0	2.00	-	-
0.4	0.71	64.33	0.6433
0.8	0.56	71.62	0.7126
1	0.43	78.23	0.7823
1.2	0.34	82.52	0.8252
1.4	0.31	84.21	0.8421
Temperature (k) = 333.15			
0	4.52	-	-
0.2	1.07	76.25	0.7625
0.4	0.93	79.38	0.7938
0.6	0.74	83.25	0.8325
0.8	0.56	87.50	0.8750
Temperature (k) = 348.15			
0	9.02	-	-
0.1	1.86	79.28	0.7928
0.2	1.50	83.34	0.8334
0.3	1.13	87.43	0.8743
0.4	0.90	89.92	0.8992

JCSE The Journal of Corrosion Science and Engineering
ISSN 1466-8858 Volume 14, Preprint 23 submitted 3 June 2011

Table 2

Impedance parameters of N80 API steel in regular mud acid (HCL/HF 12/3 wt %) at 28, 40, 60 and 75°C containing different concentrations of henna extract.

Medium (g/l)	R_P (Ω)	f_{max} (Hz)	C_{dl}(μF/cm^2)	IE(%)
		Temperature = 301.15 K		
0.0	8.500	51.8	240.66	-
0.2	20.93	21.2	239.04	59.40
0.4	24.09	37.3	120.82	64.72
0.6	27.71	37.3	102.69	69.33
0.8	28.77	37.3	99.05	70.45
1.0	33.57	37.3	84.75	74.68
1.2	36.86	37.3	72.20	76.94
1.4	41.55	37.3	68.48	79.54
1.6	45.00	37.3	63.245	81.11
		Temperature (k) = 313.15		
0.0	4.70	65.5	351.48	-
0.4	13.70	49.4	156.33	66.34
0.8	15.16	49.4	141.74	69.58
1.0	27.75	37.3	102.55	83.38
1.2	35.00	37.3	80.43	86.50
1.4	37.31	84.21	33.787	87.29
		Temperature (k) 15=333.15		
0	2.02	115.1	455.54	-
0.2	8.74	86.90	139.463	78.20
0.4	9.85	86.90	124.02	80.78
0.6	10.891	65.50	148.812	82.55
0.8	12.62	65.50	130.70	84.00
		Temperature (k) 15=348.15		
0	0.65	268.3	607.50	-
0.1	4.237	115.1	218.038	84.62
0.2	4.469	115.1	189.423	86.62
0.3	6.399	115.1	144.132	89.82
0.4	9.09	115.1	101.363	92.84

JCSE The Journal of Corrosion Science and Engineering
ISSN 1466-8858 Volume 14, Preprint 23 submitted 3 June 2011

Table 3

Kinetic parameters of N80 API steel in regular mud acid (HCL/HF 12/3 wt %) at 28, 40, 60 and75 ± 1°C containing optimum concentrations of henna extract and blank acid.

Temperature (k)	Henna concentration (g/l)	$-\beta_C$ (mV/dec)	E_{Corr} (mV/SCE)	I_{Corr} (mA/cm^2)	IE (%)
301.15	0	120	-450	1.533	-
301.15	1.6	117	-333	0.113	92.62
313.15	0	140	-415	1.933	-
313.15	1.4	122	-414	0.193	90.15
333.15	0	160	-447	5.333	-
333.15	0.8	103	-345	0.280	94.74
348.15	0	160	-430	12.001	-
348.15	0.4	140	-361	0.600	95.01

JCSE The Journal of Corrosion Science and Engineering
ISSN 1466-8858 Volume 14, Preprint 23 submitted 3 June 2011

Table 4

Surface coverage, equilibrium constant and thermodynamic parameters for the adsorption of henna on N80 API steel surface in regular mud acid (HCL/HF 12/3 %) at different temperatures.

Temperature (k)	K (g/l)	Slope	∞G_{ads} (KJ/mol)	∞H_{ads} (KJ/mol)	∞S_{ads} (J/mol)
301.15	6.37	1.131	-14.692	37.76	172
313.15	7.87	1.108	-15.828	37.76	172
333.15	17.85	1.085	-19.107	37.76	172
348.15	47.61	1.070	-22.807	37.76	172

JCSE The Journal of Corrosion Science and Engineering
ISSN 1466-8858 Volume 14, Preprint 23 submitted 3 June 2011

Table 5

Activation parameters for N80 API steel corrosion in regular mud acid solutions containing different concentrations of henna extract.

Medium (g/l)	Ea (KJ/mol)	∞H^* (KJ/mol)	∞S^* (J/mol)
0.0	27.74	28.56	-90.10
0.4	12.47	9.93	-159.22
0.8	6.849	4.17	-180.27

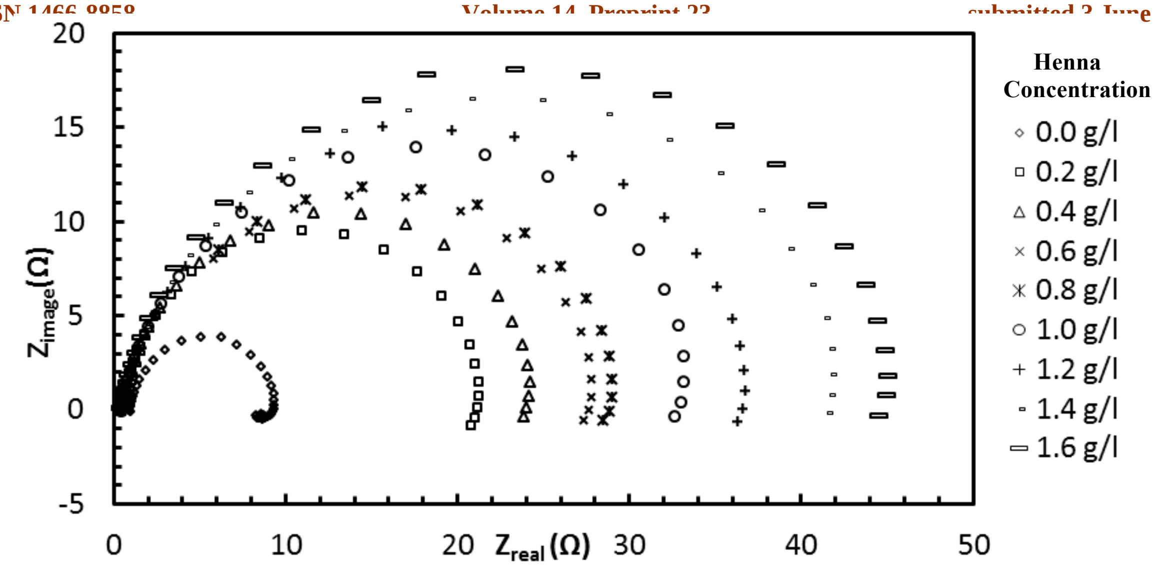

Fig. 1. Nyquist plots for N80 API steel in regular mud acid (HCL/HF 12/3 wt %) at 28 °C containing different concentrations of henna extract.

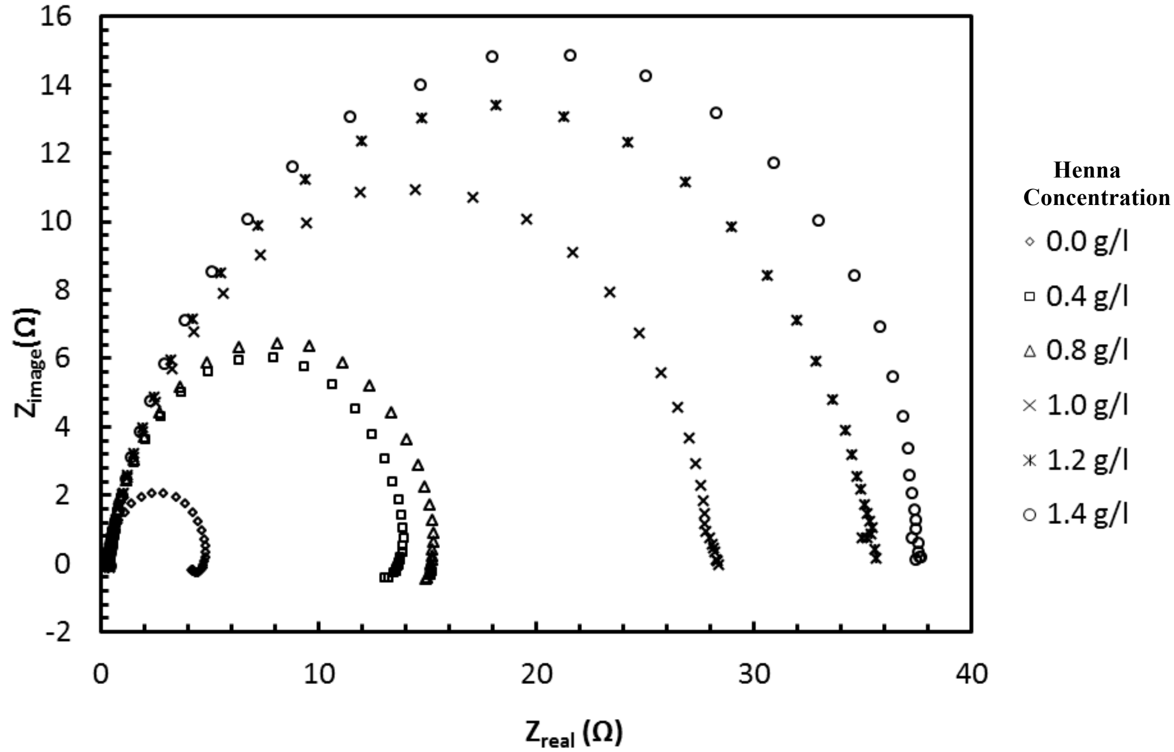

Fig. 2. Nyquist plots for N80 API steel in regular mud acid (HCL/HF 12/3 wt %) at 40 ºC containing different concentrations of henna extract.

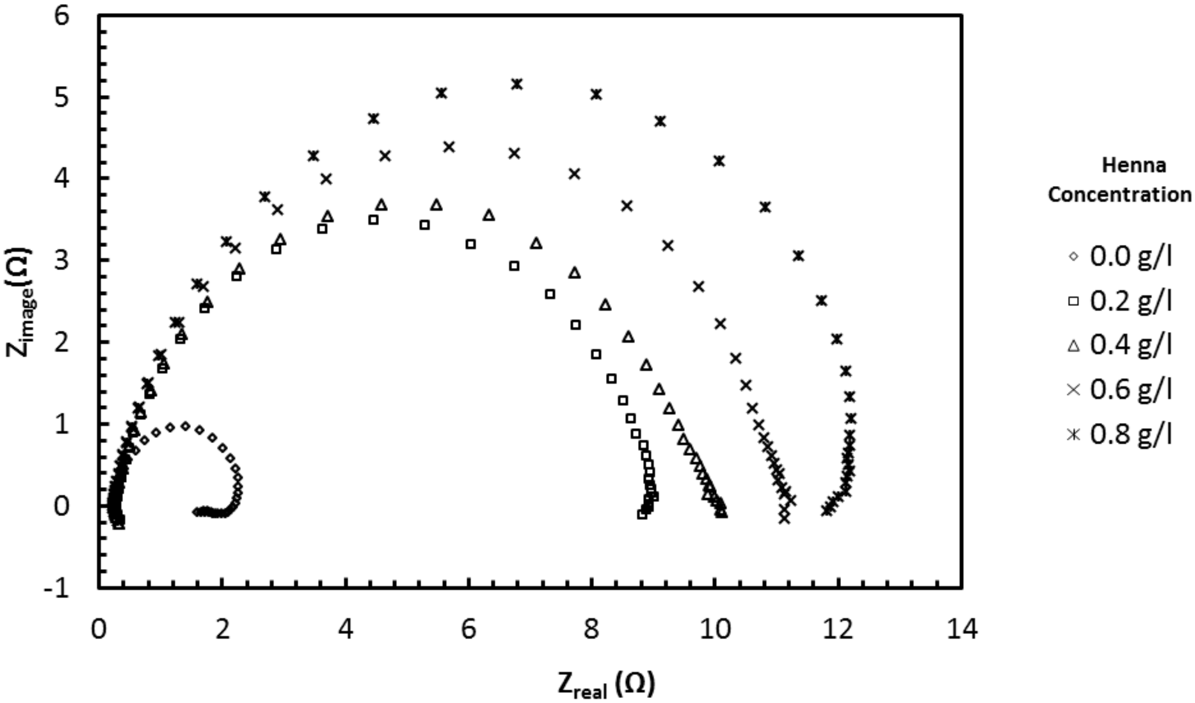

Fig. 3. Nyquist plots for N80 API steel in regular mud acid (HCL/HF 12/3 wt %) at 60 ºC containing different concentrations of henna extract.

JCSE The Journal of Corrosion Science and Engineering
ISSN 1466-8858 Volume 14, Preprint 23 submitted 3 June 2011

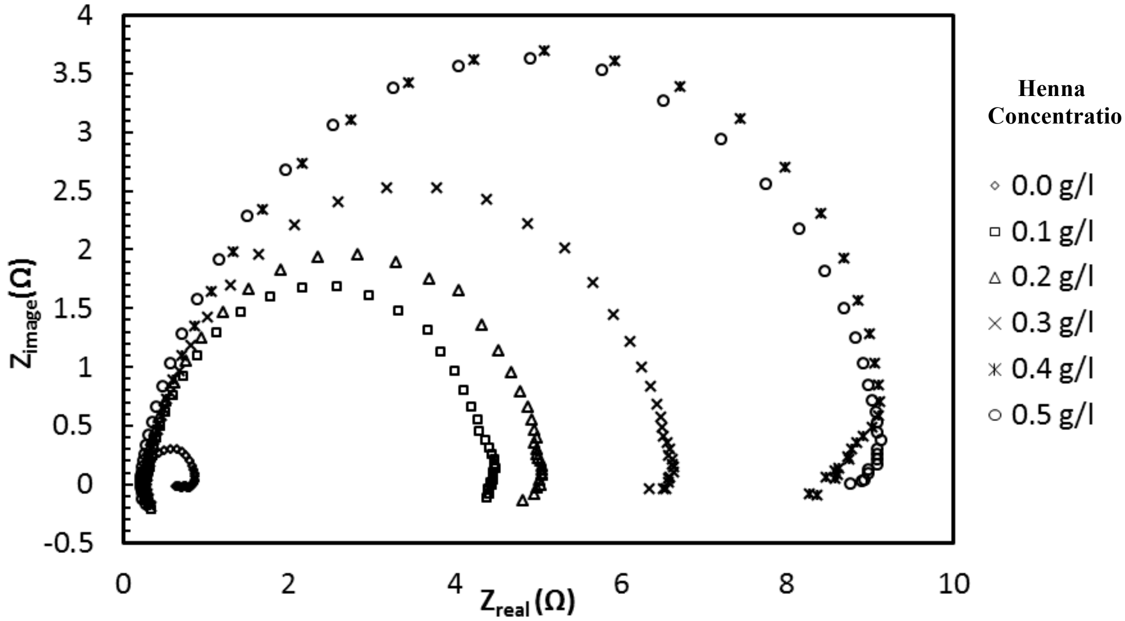

Fig. 4. Nyquist plots for N80 API steel in regular mud acid (HCL/HF 12/3 wt %) at 75 ºC containing different concentrations of henna extract.

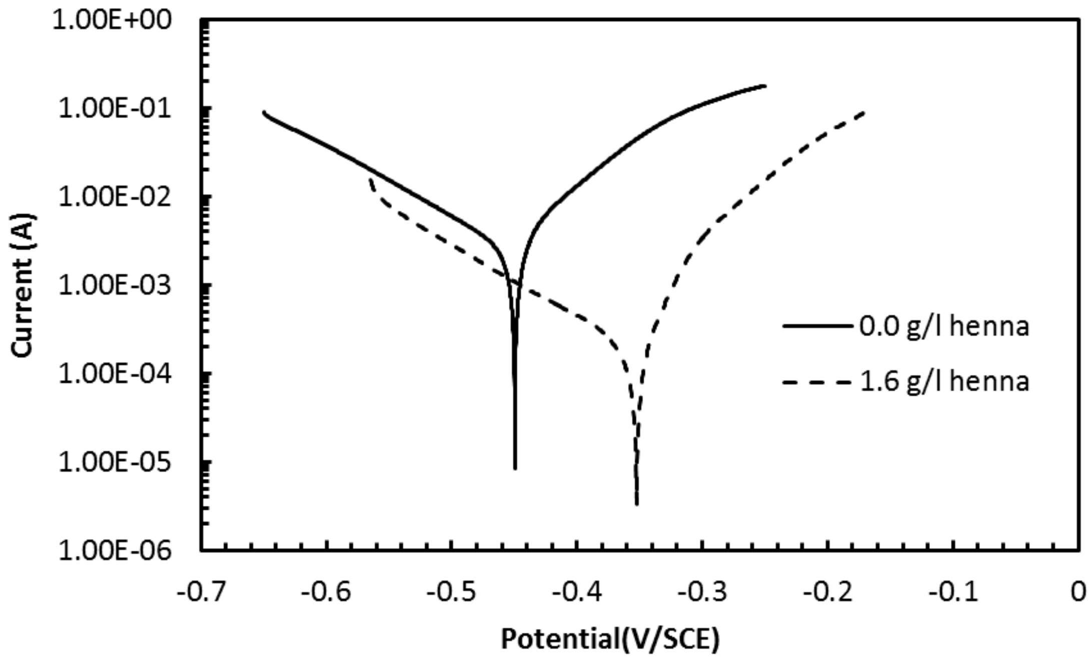

Fig. 5. Polarization curves for N80 API steel in regular mud acid (HCL/HF 12/3 wt %) in the absence and presence of optimum concentration of henna extract (1.6 g/l) at 28 ºC.

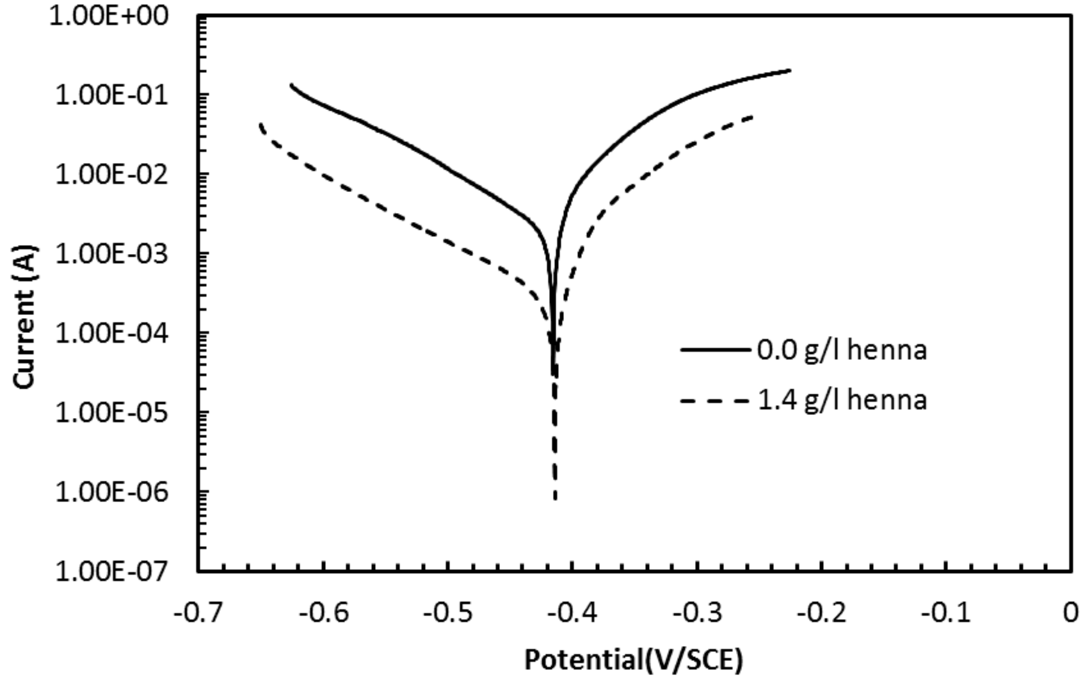

Fig. 6. Polarization curves for N80 API steel in regular mud acid (HCL/HF 12/3 wt %) in the absence and presence of optimum concentration of henna extract (1.4 g/l) at 40 ºC.

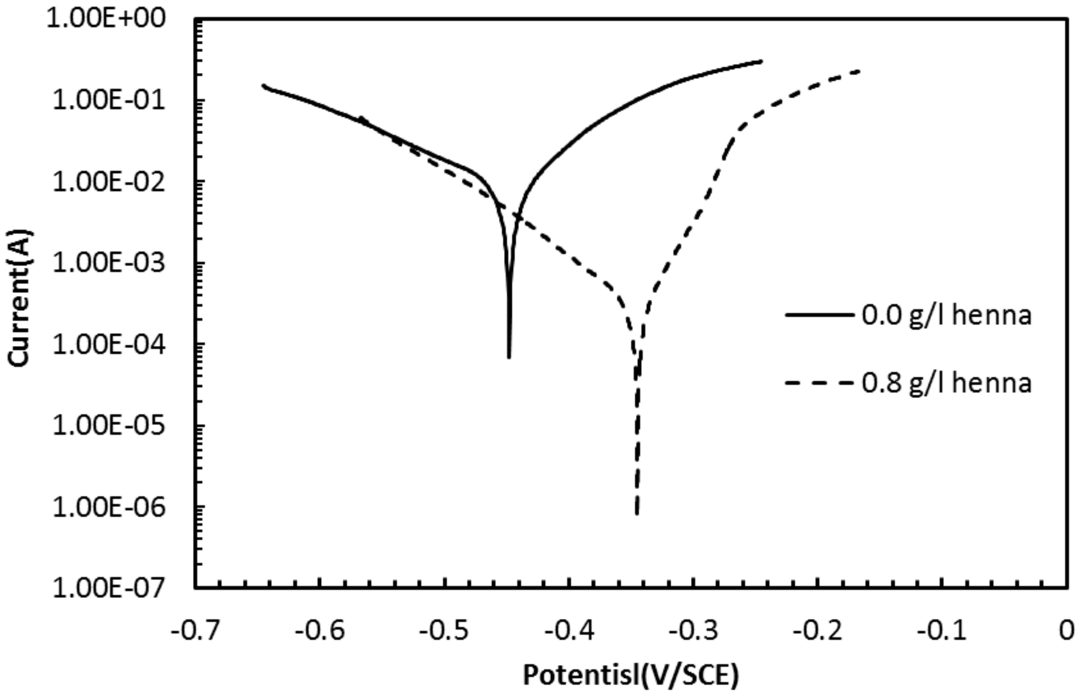

Fig. 7. Polarization curves for N80 API steel in regular mud acid (HCL/HF 12/3 wt %) in the absence and presence of optimum concentration of henna extract (0.8 g/l) at 60 ºC.

JCSE The Journal of Corrosion Science and Engineering
ISSN 1466-8858 Volume 14, Preprint 23 submitted 3 June 2011

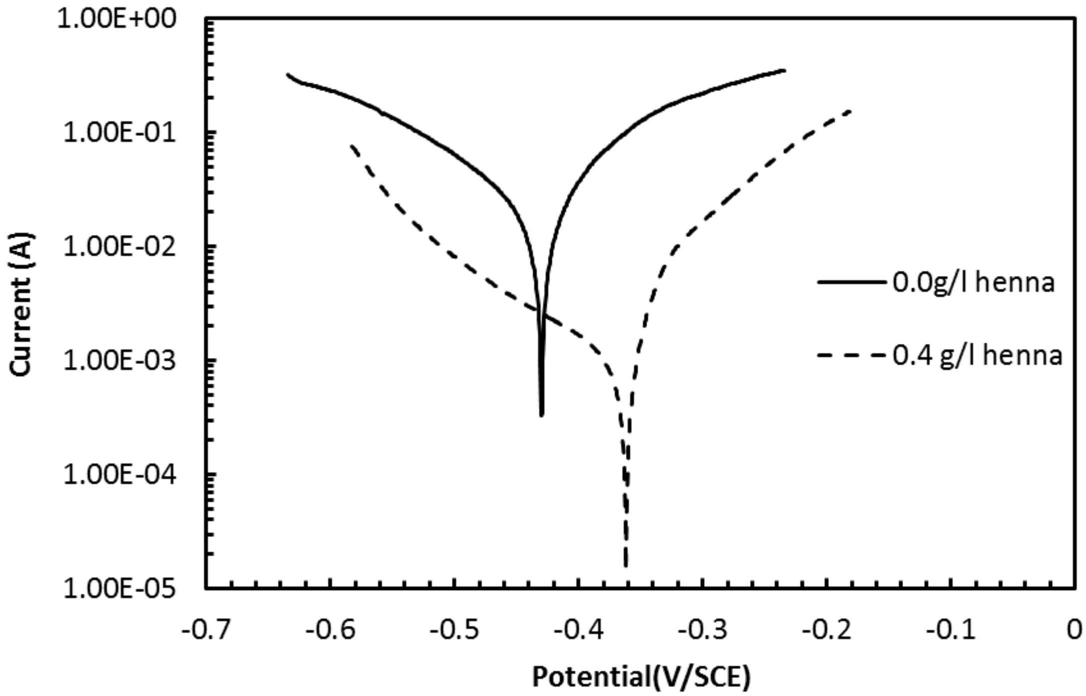

Fig. 8. Polarization curves for N80 API steel in regular mud acid (HCL/HF 12/3 wt %) in the absence and presence of optimum concentration of henna extract (0.4 g/l) at 75 ºC.

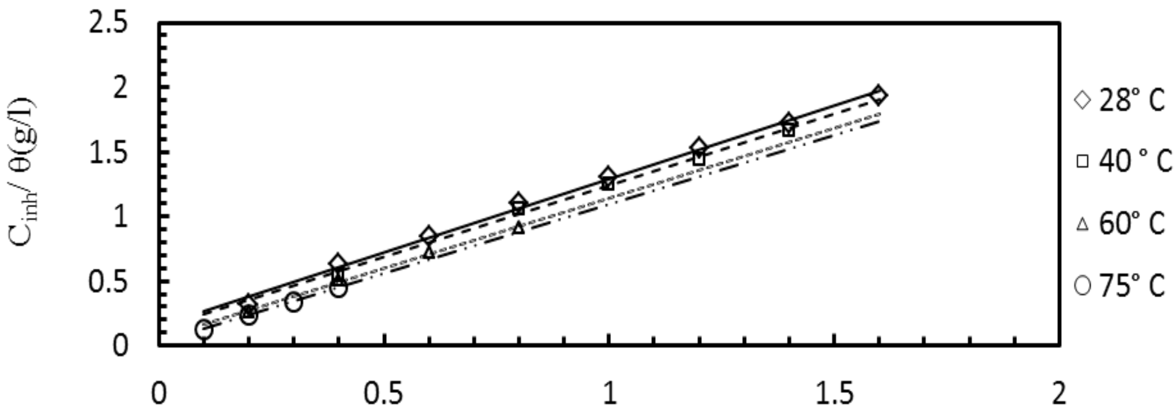

Fig. 9. Adsorption isotherm of henna on N80 API steel surface in regular mud acid (HCL/HF 12/3wt %) solution at different temperatures.

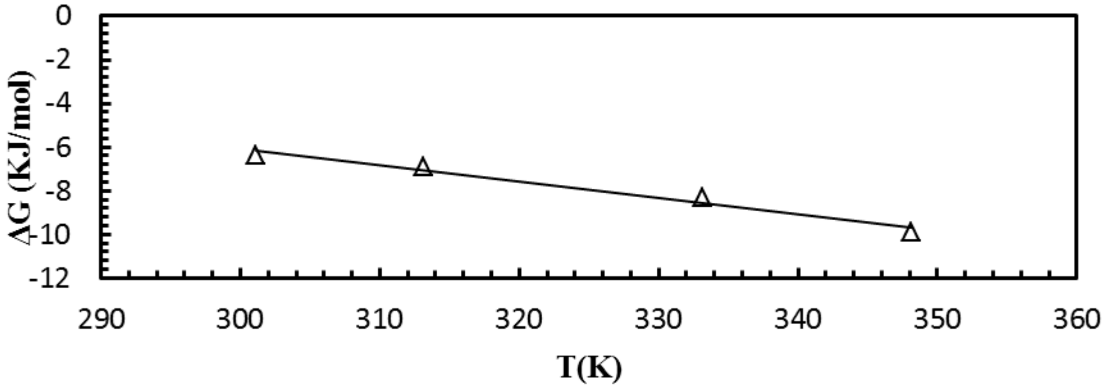

Fig. 10. Variation of ΔG_{ads} versus *T* on N80 API steel in regular mud acid (HCL/HF 12/3 wt %) containing different values of henna extract.

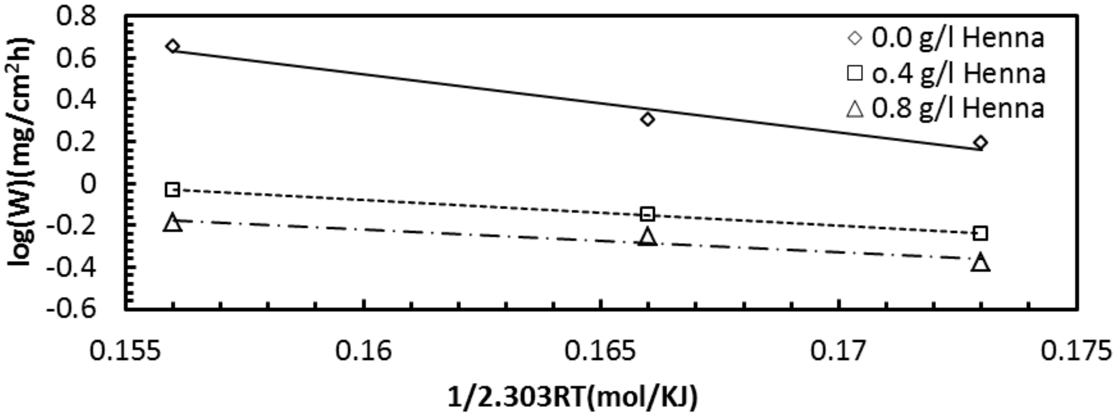

Fig. 11. Arrhenius plots of the corrosion rate for N80 API steel in regular mud acid (HCL/HF 12/3 wt %) solution.

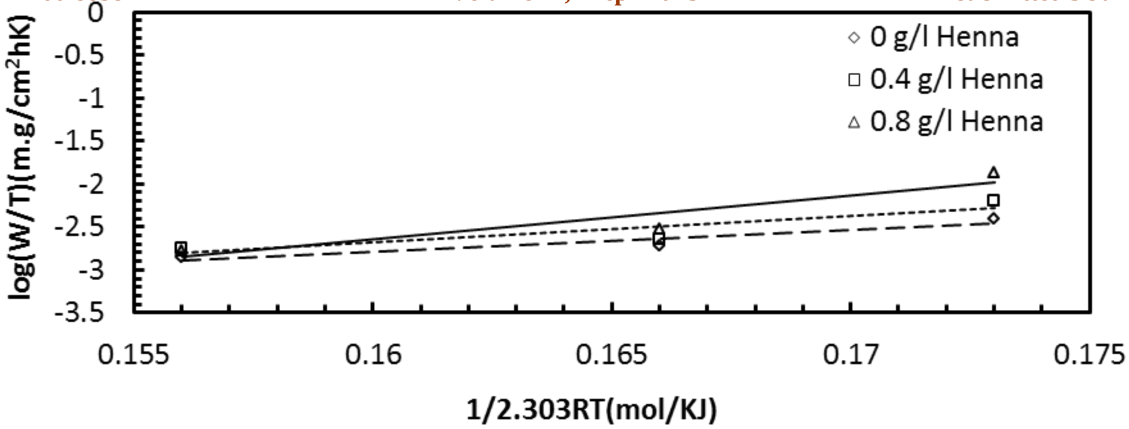

Fig. 12. Arrhenius plots of the corrosion rates in regular mud acid

ISSN 1466-8858 Volume 14, Preprint 23 submitted 3 June 2011

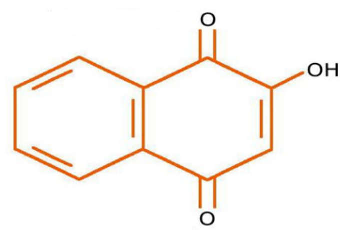

Scheme 1: Lawsone structure ($C_{10}H_6O_3$).

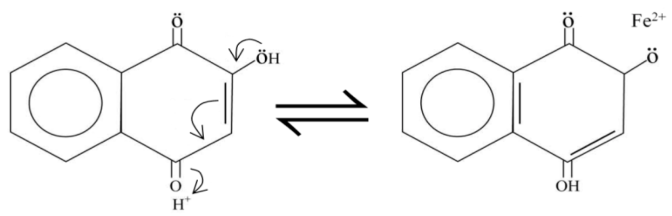

Scheme 2: Rearrangement of Lawason structure in the presence of metal cations.